

# Lymphocyte–HEV Interactions in Lymph Nodes of a Sulfotransferase-deficient Mouse

Annemieke van Zante,<sup>1</sup> Jean-Marc Gauguet,<sup>2</sup> Annette Bistrup,<sup>1</sup> Durwin Tsay,<sup>1</sup> Ulrich H. von Andrian,<sup>2</sup> and Steven D. Rosen<sup>1</sup>

<sup>1</sup>Department of Anatomy, Program in Immunology, Cardiovascular Research Institute, University of California, San Francisco, San Francisco, CA 94143

<sup>2</sup>The CBR Institute for Biomedical Research, Inc., Department of Pathology, Harvard Medical School, Boston, MA 02115

## Abstract

The interaction of L-selectin expressed on lymphocytes with sulfated sialomucin ligands such as CD34 and GlyCAM-1 on high endothelial venules (HEV) of lymph nodes results in lymphocyte rolling and is essential for lymphocyte recruitment. HEC-GlcNAc6ST-deficient mice lack an HEV-restricted sulfotransferase with selectivity for the C-6 position of N-acetylglucosamine (GlcNAc). HEC-GlcNAc6ST<sup>-/-</sup> animals exhibit faster lymphocyte rolling and reduced lymphocyte sticking in HEV, accounting for the diminished lymphocyte homing. Isolated CD34 and GlyCAM-1 from HEC-GlcNAc6ST<sup>-/-</sup> animals incorporate ~70% less sulfate than ligands from wild-type animals. Furthermore, these ligands exhibit a comparable reduction of the epitope recognized by MECA79, a function-blocking antibody that reacts with L-selectin ligands in a GlcNAc-6-sulfate-dependent manner. Whereas MECA79 dramatically inhibits lymphocyte rolling and homing to lymph nodes in wild-type mice, it has no effect on HEC-GlcNAc6ST<sup>-/-</sup> mice. In contrast, *in vitro* rolling on purified GlyCAM-1 from HEC-GlcNAc6ST<sup>-/-</sup> mice, although greatly diminished compared with that on the wild-type ligand, is inhibited by MECA79. Our results demonstrate that HEC-GlcNAc6ST contributes predominantly, but not exclusively, to the sulfation of HEV ligands for L-selectin and that alternative, non-MECA79-reactive ligands are present in the absence of HEC-GlcNAc6ST.

Key words: lymphocyte homing • L-selectin • sulfotransferase • endothelium • MECA79

## Introduction

Lymphocyte rolling, the first step of lymphocyte recruitment to lymph nodes, is mediated by the interaction of L-selectin expressed on lymphocytes with glycoprotein ligands expressed by high endothelial cells (HEC). Rolling is essential for subsequent lymphocyte activation through G-protein-coupled receptors, firm adherence of the lymphocyte, and its transmigration into the underlying lymph node parenchyma (for review see 1, 2).

All known L-selectin ligands expressed in mouse peripheral lymph nodes are reactive with the function-blocking monoclonal antibody MECA79 and are collectively called peripheral lymph node addressin (PNAd) (3). In human tonsils, CD34, podocalyxin, and endomucin, in addition to other molecularly unidentified ligands, comprise the PNAd complex (4–6). In the mouse, four HEV-expressed proteins

that carry the MECA79 epitope have been identified: GlyCAM-1, CD34, Sgp200, and endomucin (6, for review see 7). These glycoprotein ligands are all sialomucins (7). CD34 is a transmembrane protein (8), whereas GlyCAM-1 is a peripheral membrane protein found both associated with HEC and as a secreted molecule in serum (9).

L-selectin functions as a C-type lectin, its binding being critically dependent on the appropriate posttranslational modification of its endothelial ligands (7). As detailed below, L-selectin recognizes sialyl Lewis X (sLex) modified with GlcNAc-6-sulfate (6-sulfo-sLex). The importance of sialylation of the ligands has been demonstrated both *in vitro* and *in vivo* (10, 11). The critical participation of fucosylation

*Abbreviations used in this paper:* FucT, fucosyltransferase; GlcNAc, N-acetylglucosamine; HEC, high endothelial cell; HEC-GlcNAc6ST, HEC-GlcNAc-6-sulfotransferase; HEV, high endothelial venule; LSST, L-selectin ligand sulfotransferase; OSGE, O-sialoglycoprotein endopeptidase; PNAd, peripheral node addressin; sLex, sialyl Lewis X.

Address correspondence to Steven D. Rosen, Box 0452, University of California, San Francisco, CA 94122. Phone: (415) 476-1579; Fax: (415) 476-4845; email: sdr@itsa.ucsf.edu

in lymphocyte homing has been established through the analysis of mice deficient in two  $\alpha$ 1,3-fucosyltransferases, FucT-IV and FucT-VII (12). The contribution of sulfation was first demonstrated using chlorate, a metabolic inhibitor of sulfation (13, 14). Biochemical analysis of mouse GlyCAM-1 and CD34 revealed that GlcNAc-6-SO<sub>4</sub> comprises at least 50% (15, unpublished data) of the sulfated saccharides, whereas it makes up >90% of the sulfated saccharides within human tonsillar ligands (16). A structural analysis first revealed that 6-sulfo-sLex (sialyl Lewis x modified with GlcNAc-6-SO<sub>4</sub>) to be a major capping group of the O-linked chains of GlyCAM-1 (17), a finding that was confirmed in human with a panel of mAbs (18).

These results stimulated interest in the GlcNAc-6-O-sulfotransferase responsible for the L-selectin ligand modification. One enzyme discovered through these efforts has an expression pattern highly restricted to HEV. Independently cloned by two groups, this enzyme is known alternatively as HEC-GlcNAc6ST (19) or L-selectin ligand sulfotransferase (LSST) (20). In reconstitution experiments, GlyCAM-1-IgG coexpressed with HEC-GlcNAc6ST and FucT-VII supports greater rolling of L-selectin<sup>+</sup> cells than GlyCAM-1-IgG expressed with FucT-VII alone (21). Similar results were obtained with CD34 (20).

The MECA79 antibody has proven a useful tool in the elucidation of the mechanisms of lymphocyte rolling and recruitment. It was originally identified based on its ability to inhibit the L-selectin mediated attachment of lymphocytes to HEV in lymph node sections as well as the homing of lymphocytes to peripheral lymph nodes (3). Subsequent intravital microscopy studies established that MECA79 potently blocks the initial tethering and rolling of lymphocytes in peripheral lymph node HEV (22). Biochemically, MECA79 cross-reacts in a function-blocking manner with the same complex of mucins (PNAd) recognized by L-selectin (14, 23). The MECA79 epitope requires GlcNAc-6-sulfate in the context of an extended Core1 structure (24, 25).

To determine the role of HEC-GlcNAc6ST in vivo, we have generated mice deficient in the enzyme (26). Our initial characterization showed that the in vitro binding of lymphocytes to lymph node HEV and luminal staining of HEV by an L-selectin chimera are eliminated in the null mice (26). Additionally, MECA79 reactivity of HEV is greatly diminished, with the residual staining being most apparent on the abluminal aspect of these venules. In a short-term assay, the ability of lymphocytes to home to lymph nodes in vivo in HEC-GlcNAc6ST<sup>-/-</sup> mice is 50% of that in wild-type mice. The residual homing in null mice is entirely L-selectin dependent. Given the observed decrease in luminal MECA79 reactivity, yet the retention of L-selectin dependent homing, we proposed two classes of luminal ligands for L-selectin. In wild-type mice, lymphocyte rolling is dependent on relatively high affinity, MECA79-reactive ligands that we have termed class 1 ligands. We proposed that in null mice rolling is supported by a MECA79-unreactive class 2 ligand. This class 2 ligand is presumably of lower affinity or lower abundance than class 1, since it does not stain with an L-selectin-IgM chi-

mera. The question of whether the class 2 ligand is simply undersulfated class 1 ligands or a qualitatively distinct ligand remained unanswered in our previous study.

To further our understanding of the contribution of HEC-GlcNAc6ST to lymphocyte homing, we have undertaken a detailed study of lymphocyte rolling in vivo as well as a biochemical and biophysical characterization of L-selectin ligands produced by HEC-GlcNAc6ST null mice.

## Materials and Methods

**Intravascular Staining with MECA79.** The MECA79 reactivity of the luminal aspect of HEV was assessed by injecting 50  $\mu$ g of MECA79 (rat IgM) in 100  $\mu$ l of PBS into tail veins of HEC-GlcNAc6ST<sup>-/-</sup> and <sup>+/+</sup> mice. After 30 min mice were killed and PN dissected out. PN were snap-frozen in OCT and cryostat sections were stained with 1.5  $\mu$ g/ml Cy3-conjugated goat  $\alpha$ -rat IgM (Jackson ImmunoResearch Laboratories) and processed for immunofluorescence.

**In Vivo Homing.** Lymphocyte homing in vivo was performed according to published procedures (26). Briefly, HEC-GlcNAc6ST<sup>-/-</sup> and <sup>+/+</sup> mice were pretreated with 75  $\mu$ g of mAb MECA79 or PBS injected into tail veins. 1 h later, mouse MN lymphocytes ( $1.7 \times 10^7$ ) labeled with 5 mM 5-chloromethylfluorescein diacetate (CMFDA, Cell-Tracker; Molecular Probes) were injected. 1 h after cells were injected, recipient mice were killed, and PN (auxiliary and brachial nodes) were dissected out. Fractional content of fluorescent cells was determined by flow cytometry (FACScan, Becton Dickinson) (500,000 cells per organ). To assess the effect of MECA79 on homing, the data were normalized for each animal (fractional value of CMFDA positive cells divided by the mean of the fractional values for all of the PBS-injected mice of the same genotype within the experiment). Data from two separate experiments were pooled, with a total of five (<sup>+/+</sup>) or nine (<sup>-/-</sup>) animals per group.

**Intravital Microscopy.** Intravital microscopy of the murine inguinal peripheral lymph node was performed as described (22, 27). Briefly, young adult (6–12 wk) HEC-GlcNAc6ST<sup>-/-</sup> or <sup>+/+</sup> controls were anesthetized by intraperitoneal injection of 10 ml/kg of saline containing xylazine (1 mg/ml) and ketamine (5 mg/ml). A skin incision was made to expose the inguinal lymph node. Calcein-labeled lymphocytes injected into a right femoral artery catheter were visualized in LN microvasculature by intravital epifluorescence microscopy (IV-500; Micron Instruments) with a video-triggered xenon arc stroboscope (Chadwick-Helmuth) and recorded on a Hi8 VCR (Sony). Offline video analysis was performed as described previously (28). Rolling fraction is measured as the percent of fluorescent cells interacting with the vessel wall relative to the total number of fluorescent cells passing through the vessel during the observation period. The sticking fraction is defined as the percent of rolling fluorescent cells that arrest on the vessel wall for  $\geq 30$  s. Velocity analysis was performed using PC software capable of random line-length measurements (29). The velocity of  $\geq 10$  rolling and 20 noninteracting cells were measured for each venule to obtain mean fast cell velocity ( $V_{fast}$ ), blood flow velocity ( $V_{blood}$ ), and rolling velocity ( $V_{roll}$ ) as described previously (28). To correct for the effect of varying  $V_{blood}$  on  $V_{roll}$ , we calculated the relative rolling velocity ( $V_{rel}$ ) according to the formula  $V_{rel} = V_{roll}/V_{blood} \times 100\%$ .

All data are shown as mean  $\pm$  SEM, unless otherwise noted. Rolling and sticking fractions were compared using an unpaired Student's *t* test. Statistical analysis of velocity histograms was per-

formed using the Mann-Whitney test and the Kolmogorov-Smirnov test. Differences were considered statistically significant when  $P < 0.05$ .

**Isolation and Analysis of Sulfated Ligands.** Equal masses of mesenteric and PN were harvested from HEC-GlcNAc6ST<sup>-/-</sup> and <sup>+/+</sup> mice and minced. About 0.5 g of LN tissue was incubated in 2 ml of sulfate-free RPMI 1640 supplemented with HEPES buffer, penicillin/streptomycin, and 2 mCi Na<sup>35</sup>SO<sub>4</sub> (ICN) overnight in a cell-culture incubator. GlyCAM-1 was isolated by immunoprecipitation from the conditioned medium with 20 μg CAMO2 (antipeptide 2 polyclonal Ab) (30). CD34 was isolated by immunoprecipitation from clarified precleared lysates of tissue pieces with 10 μg RAM34 mAb (PharMingen). Immunoprecipitates were quantified by Western blotting with CAMO5 (antipeptide 5 polyclonal Ab) (30) or a polyclonal antibody directed to murine CD34 (31). MECA79 reactivity was quantified by Western blotting and densitometry. Sulfate incorporation was determined by autoradiography and densitometry.

**Purification of GlyCAM-1 from Serum.** GlyCAM-1 was purified from serum essentially as described (32). Briefly, 20 ml of se-

rum from HEC-GlcNAc6ST<sup>-/-</sup> or <sup>+/+</sup> mice was extracted with chloroform:methanol (4:1), dialyzed overnight against PBS, clarified by centrifugation, and precleared with protein A before precipitation with CAMO2 bound to protein A. GlyCAM-1 was recovered by incubating beads with 1 mg/ml CAMO2 peptide, separated from eluting peptide by extensive washing, and concentrated using Centricon-30 filter concentrators (Amicon).

**ELISAs.** To equalize coating densities of serum-derived GlyCAM-1, ELISAs were performed. Protein was coated onto 96-well Immulon-2 plates (Dynex Labs) and detected with biotinylated anti-GlyCAM-1 peptide Ab (5) (30) followed by streptavidin-conjugated alkaline phosphatase. MECA79 reactivity was determined using biotinylated MECA79 (Ligocyte Pharmaceuticals). L-selectin-IgM was prepared as described by Bistrup (19). E-selectin-IgM and P-selectin-IgM chimeras, produced according to published procedures (33), were provided by Dr. Lloyd Stoolman. Fucosylation was detected using *Aleuria aurantia* lectin (AAL-biotin, Vector) with inhibition by 50 mM fucose (Sigma-Aldrich).

**Flow Chamber Analysis.** For these experiments, polystyrene dishes coated with serum-derived GlyCAM-1 in Tris-buffered

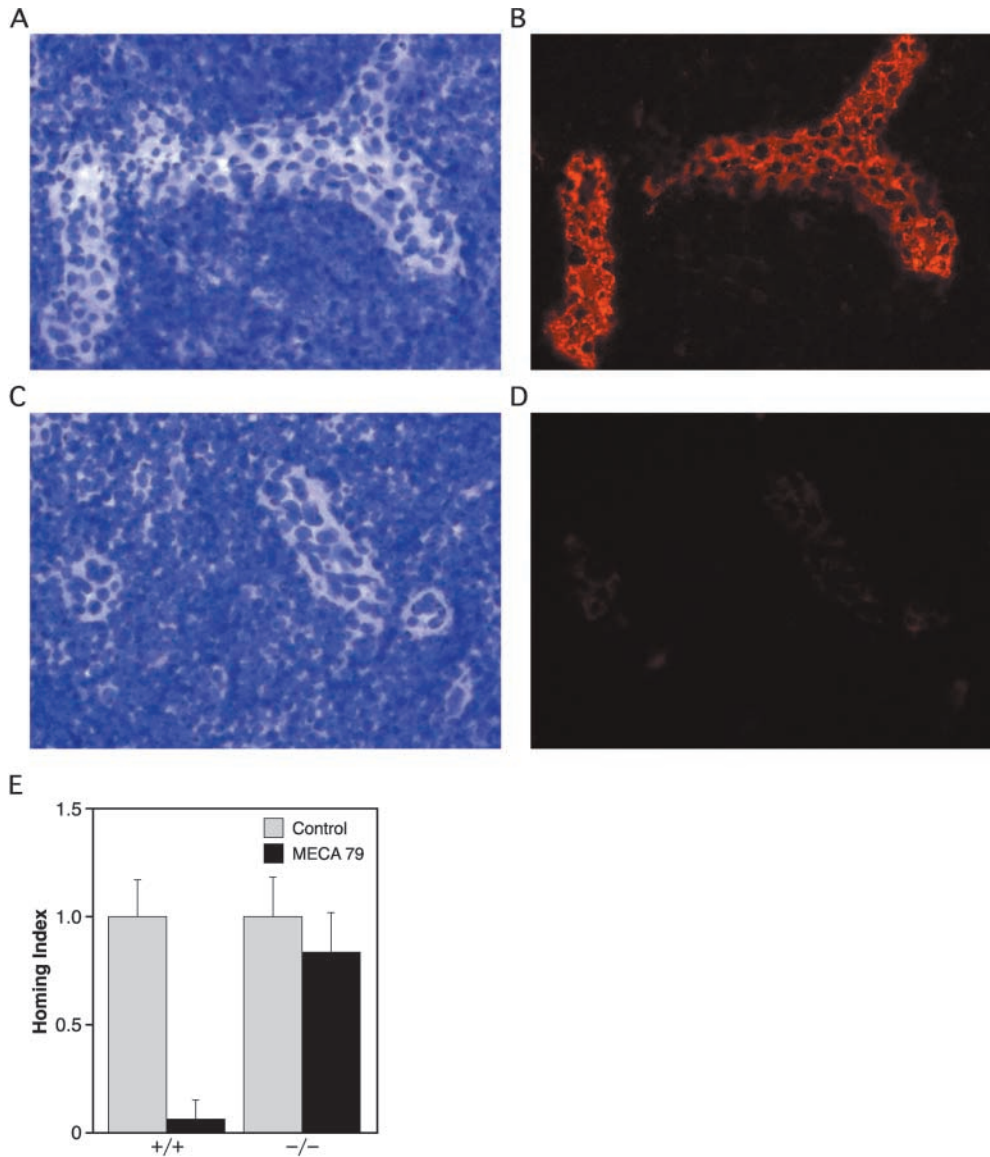


**Figure 1.** Intravascular staining with MECA79 and effect on in vivo homing. (A–D) MECA79 mAb was injected intravenously into HEC-GlcNAc6ST<sup>-/-</sup> or <sup>+/+</sup> mice. 30 min later peripheral lymph nodes were dissected out and processed for immunofluorescence microscopy. Bright field images of <sup>+/+</sup> (A) and <sup>-/-</sup> (C) lymph nodes. Intravascular staining with MECA79 of (B) <sup>+/+</sup> and (D) <sup>-/-</sup> HEV. Magnification 200×. (E) MECA79 mAb or PBS was injected intravenously into HEC-GlcNAc6ST<sup>-/-</sup> or <sup>+/+</sup> mice and the homing of fluorescently labeled cells was determined and normalized to produce a homing index as described in Materials and Methods. Consistent with our previous findings (26), homing in the HEC-GlcNAc6ST<sup>-/-</sup> mice was 59% relative to homing in wild-type.

saline, pH 9, overnight at 4°C. Blocked dishes were incorporated as the lower wall of a parallel plate flow chamber (34). Human Jurkat T cells or 38C13 murine lymphoma cells were perfused through the flow chamber at  $1-2 \times 10^6$  cells/ml. The number of rolling cells and rolling velocity was determined as described in (34). For inhibition studies, cells were pretreated with 5  $\mu\text{g/ml}$  DREG56 (Caltag) or resuspended in  $\text{Ca}^{2+}/\text{Mg}^{2+}$ -free HBSS with 5mM EDTA. For sialidase inhibition, coated substrates were treated with 10 mU/ml *Vibrio cholera* sialidase (Glyko) for 30 min at RT. For MECA79 inhibition experiments, coated substrates were incubated with MECA79 after the usual blocking step.

## Results

**Intravascular Staining with MECA79.** We had previously observed by conventional staining of sections that HEV of HEC-GlcNAc6ST null mice have reduced luminal MECA79 reactivity (26). To directly assess the presence of epitopes accessible to the blood, we injected MECA79 intravenously into HEC-GlcNAc6ST<sup>-/-</sup> and +/+ mice. Animals were killed 30 min later. Cryostat sections of peripheral lymph nodes were stained for the presence of bound primary antibody. Whereas MECA79 staining was strongly associated with HEV of wild-type mice, it was very weak or undetectable on the luminal surface of HEV in HEC-GlcNAc6ST<sup>-/-</sup> mice (Fig. 1 D).

**MECA79 Inhibition of Homing in HEC-GlcNAc6ST Null Mice.** Streeter et al. (3) first reported the ability of MECA79 to inhibit homing to peripheral lymph nodes in mice. MECA79 has also been shown to substantially (>90%) inhibit L-selectin-dependent rolling in HEV by intravital microscopy (22). Since we had observed that HEC-GlcNAc6ST null mice had greatly reduced luminal MECA79 reactivity (Fig. 1 D), we wanted to determine whether MECA79 would inhibit homing of lymphocytes in these animals. We investigated this question by injecting mice with MECA79 mAb intravenously 1 h before the injection of fluorescently labeled lymphocytes. Lymphocyte homing was quantified by flow cytometry, which allowed the enumeration of the percentage of fluorescently labeled cells normalized to the total number of cells in peripheral lymph nodes. Strikingly, MECA79 had no effect on homing to lymph nodes in HEC-GlcNAc6ST null animals,

while homing in wild-type animals was almost completely inhibited (Fig. 1 E). Since the residual homing to lymph nodes in the null mice is completely dependent on L-selectin (26), these results establish that in the absence of HEC-GlcNAc6ST, L-selectin can function in lymphocyte homing to peripheral nodes independently of MECA79-reactive ligands.

**Intravital Microscopy of Peripheral Lymph Nodes of HEC-GlcNAc6ST Null Mice.** To directly observe the effect of deletion of HEC-GlcNAc6ST on the interaction of lymphocytes with HEV *in vivo*, we employed intravital microscopy. Von Andrian has described the hierarchical branching of venules within peripheral lymph nodes and defined five distinct venular orders with orders 3–5 corresponding to paracortical HEV (22). As shown in Fig. 2 A, the rolling fraction of lymphocytes was not significantly different between HEC-GlcNAc6ST<sup>-/-</sup> and wild-type mice. However, the sticking fraction of lymphocytes was significantly diminished in null mice (Fig. 2 B). While the sticking fraction was comparable in third order venules of wild-type and null mice, it was reduced to 27% ( $P < 0.0001$ ) and 19% of wild-type ( $P < 0.005$ ) in fourth and fifth order venules, respectively. Since the majority (>90%) of lymphocyte accumulation occurs in fourth and fifth order HEV (27), the observed defect in lymphocyte sticking was consistent with the observed 50% decrease in lymphocyte homing in HEC-GlcNAc6ST null mice (26).

The median velocity of lymphocyte rolling in third order venules was 43  $\mu\text{m/s}$  in wild-type mice and increased to 58  $\mu\text{m/s}$  in null mice ( $P > 0.5$ , Fig. 3 A). The difference in fourth order venules was much more dramatic, with a greater than fourfold increase from 21  $\mu\text{m/s}$  in wild-type mice to 89  $\mu\text{m/s}$  in null mice ( $P < 0.0001$ ) (Fig. 3 C). These differences could not be explained by hemodynamic factors, since the frequency distribution of rolling velocities normalized to the mean blood flow velocity in each venule ( $V_{\text{rel}}$ ) was shifted in third order (Fig. 3 B) and, especially, fourth order venules ( $P < 0.0001$ , Fig. 3 D). Velocities were not measured in fifth order venules, since the accumulation of adherent cells obscured many venule segments. Our data represent the first reported case where the velocity of lymphocyte rolling in peripheral lymph node HEV has been perturbed.

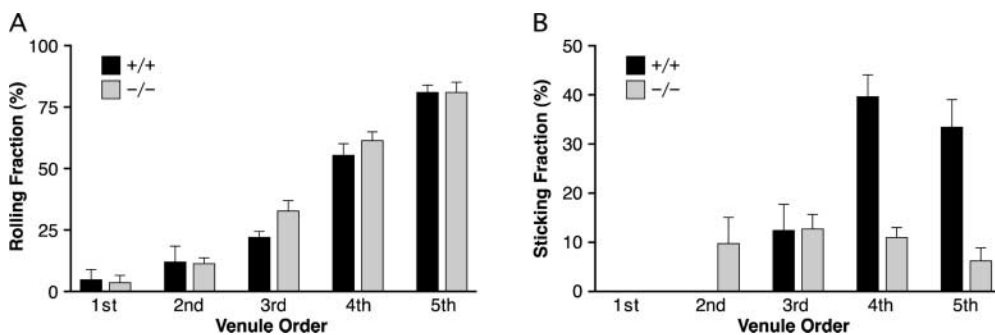


**Figure 2.** Lymphocyte rolling and sticking fractions in HEV of HEC-GlcNAc6ST<sup>-/-</sup> mice. (A) Rolling fractions were determined as the percentage of rolling cells in the total flux of fluorescently labeled lymphocytes. Data are based on four HEC-GlcNAc6ST<sup>-/-</sup> mice (1st-4; 2nd-5; 3rd-7; 4th-16; 5th-11 venules) and four +/+ mice (1st-2; 2nd-9; 3rd-12; 4th-16; 5th-7 venules). Bars represent mean  $\pm$  SEM. (B) Sticking frac-

tions were determined as the percentage of rolling cells that subsequently arrested (stationary  $\geq 30$  s). Data are based on the same four HEC-GlcNAc6ST<sup>-/-</sup> and four +/+ mice and venules indicated in A. Sticking was not observed in first order venules or in second order venules in +/+ mice.

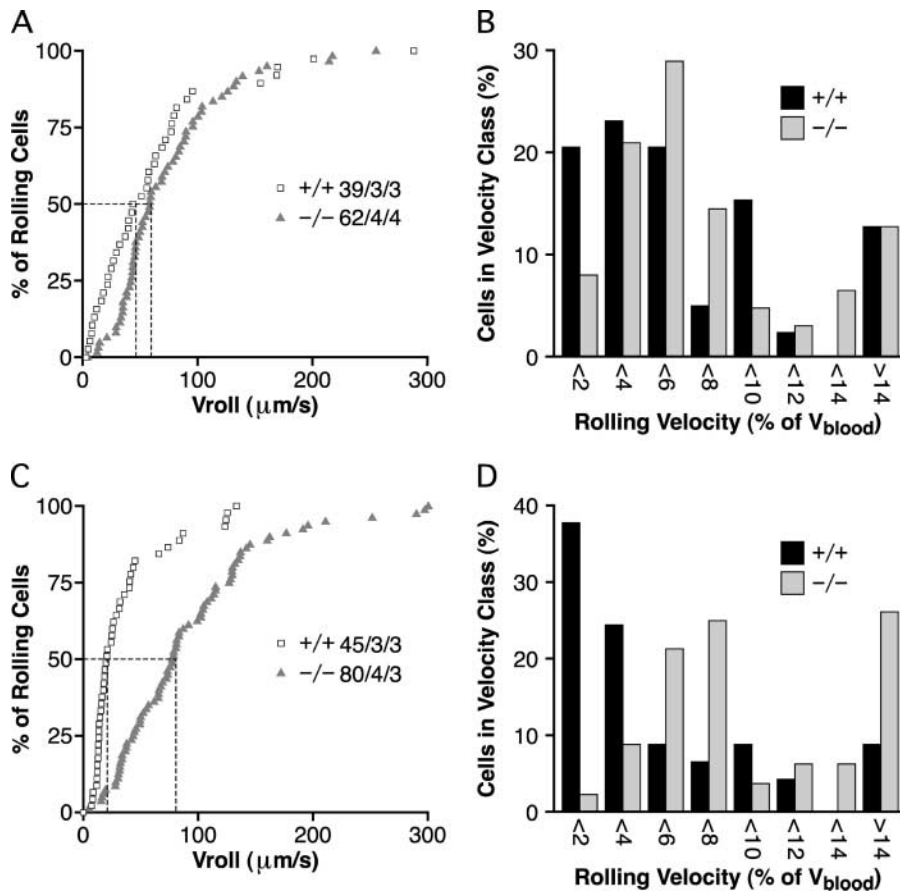


**Figure 3.** Lymphocyte rolling velocities in HEC-GlcNAc6ST<sup>-/-</sup> mice. (A and C) Cumulative rolling velocity curves for third order (A) and fourth order (C) venules. The percentage of cells that rolled at or below a given velocity is shown as a function of V<sub>roll</sub>. n = cells/venules/mice. (B and D) Distribution of V<sub>rel</sub> frequencies for third order (B) and fourth order (D) venules. V<sub>rel</sub> was calculated as described in Materials and Methods and cells were assigned to V<sub>rel</sub> classes ranging from >0 to <2%, 2% to <4%, and so on.

Since we observed that MECA79 had no effect on the ability of lymphocytes to home to lymph nodes in HEC-GlcNAc6ST null mice (Fig. 1), we expected that lymphocyte rolling in peripheral lymph node HEV would be insensitive to MECA79. To test this hypothesis, we injected mice with either MECA79 or a control rat IgM 15 min before the injection of fluorescently labeled lymphocytes. MECA79 treatment nearly eliminated rolling in wild-type mice (76–94% inhibition in second to fifth order venules), while the rolling fraction in MECA79

treated HEC-GlcNAc6ST<sup>-/-</sup> mice was unchanged (Fig. 4 A). The isotype control antibody did not affect the rolling fraction (Fig. 4 A) or sticking fraction (not depicted) in either HEC-GlcNAc6ST<sup>-/-</sup> or +/+ mice. To confirm that MECA79-resistant rolling in the null mice remained L-selectin dependent (26), we employed lymphocytes isolated from L-selectin null animals. When these cells were injected into HEC-GlcNAc6ST<sup>-/-</sup> mice that had been pretreated with MECA79, no rolling was observed (Fig. 4 B).

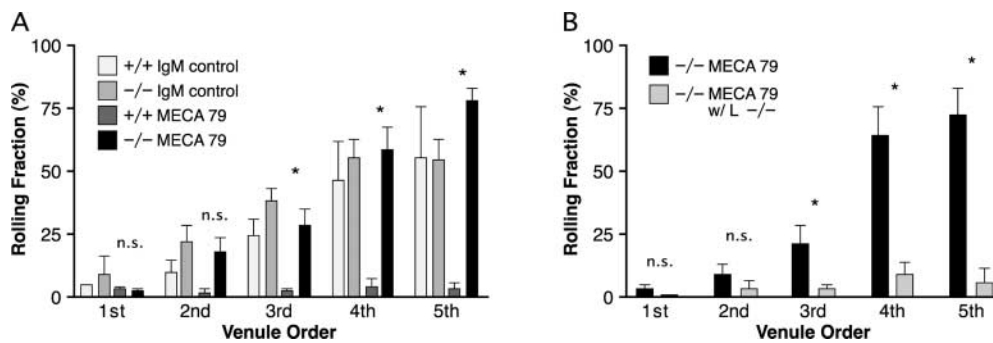


**Figure 4.** Effect of MECA79 mAb on lymphocyte rolling. (A) MECA79 mAb or isotype control rat IgM was injected via a femoral artery catheter into HEC-GlcNAc6ST<sup>-/-</sup> or +/+ mice. 15 min later, fluorescently labeled lymphocytes were injected. Data are based on 2 HEC-GlcNAc6ST<sup>-/-</sup> mice injected with rat IgM (1st-2; 2nd-5; 3rd-8; 4th-5; 5th-2 venules), two +/+ mice injected with rat IgM (1st-1; 2nd-2; 3rd-3; 4th-3; 5th-3

venules), two HEC-GlcNAc6ST<sup>-/-</sup> mice injected with MECA79 (1st-3; 2nd-6; 3rd-8; 4th-8; 5th-7 venules), and 2 +/+ mice injected with MECA79 (1st-2; 2nd-5; 3rd-8; 4th-8; 5th-5 venules). Bars represent mean ± SEM. (B) Fluorescently labeled L-selectin<sup>-/-</sup> lymphocytes were injected into HEC-GlcNAc6ST<sup>-/-</sup> mice treated with MECA79. Data are based on 4 HEC-GlcNAc6ST<sup>-/-</sup> mice injected with MECA79 (1st-3; 2nd-6; 3rd-8; 4th-9; 5th-7 venules) and one HEC-GlcNAc6ST<sup>-/-</sup> mouse injected with MECA79 and L-selectin<sup>-/-</sup> lymphocytes (1st-1; 2nd-3; 3rd-5; 4th-3; 5th-2 venules).

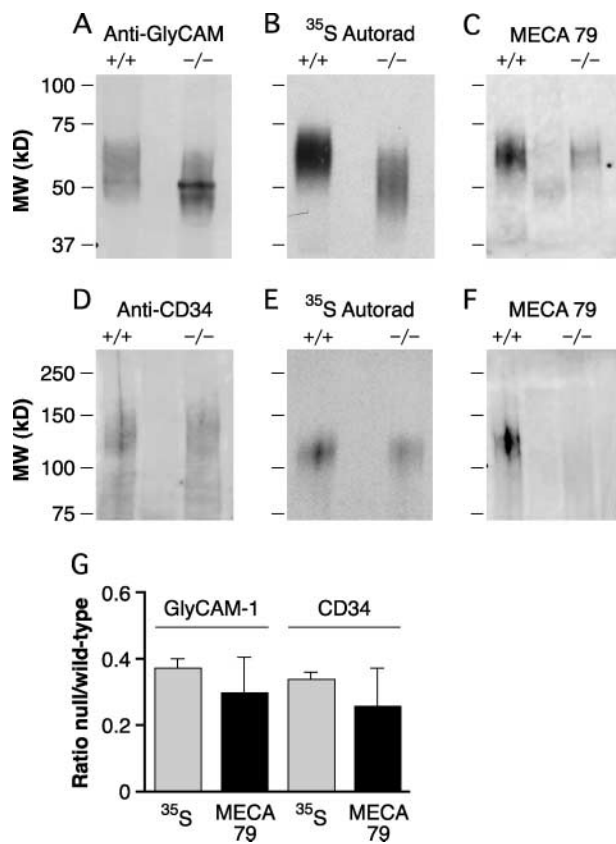


**Figure 5.** <sup>35</sup>Sulfate incorporation and MECA79 reactivity of GlyCAM-1 and CD34. (A and D) Lymph nodes from HEC-GlcNAc6ST<sup>-/-</sup> and +/+ mice were incubated with Na<sup>35</sup>SO<sub>4</sub>. Immunoprecipitated GlyCAM-1 and CD34 were separated by SDS-PAGE and transferred to PVDF for Western blotting. (A) GlyCAM-1 was detected with an antipeptide Ab (CAMO5). (D) CD34 was detected with an affinity-purified polyclonal Ab. (B and E) <sup>35</sup>S-labeled immunoprecipitated ligands GlyCAM-1 (B) and CD34 (E) detected by autoradiography. (C and F) MECA79 reactivity of GlyCAM-1 (C) and CD34 (F) detected by Western blotting. (G) Relative sulfate incorporation and MECA79 reactivity of GlyCAM-1 and CD34 from HEC-GlcNAc6ST<sup>-/-</sup> mice. <sup>35</sup>S incorporation was measured by performing densitometry on autoradiographs as shown in B and E and normalized for protein based on Western blots performed in parallel with protein-specific Abs as in A and D. MECA79 reactivity was measured by performing densitometry on Western blots shown in C and F and normalized based on protein-specific Western blots performed in parallel. Data are the means ± SEMs of three independent preparations.

**Sulfate Incorporation into L-Selectin Ligands in HEC-GlcNAc6ST Null Mice.** We had previously observed that staining of lymph node HEV by an L-selectin chimera or MECA79 was greatly diminished in HEC-GlcNAc6ST<sup>-/-</sup> animals (26), consistent with the sulfation dependency of these interactions. We wanted to confirm this association by investigating the effect of the genetic deletion of HEC-GlcNAc6ST on the degree of sulfate incorporation into isolated L-selectin ligands. <sup>35</sup>SO<sub>4</sub>-GlyCAM-1 and -CD34 were, respectively, immunoprecipitated from conditioned media and detergent lysates of metabolically labeled lymph nodes. The bands were quantified for protein by Western blotting and for sulfate incorporation by autoradiography (Fig. 5). When normalized for protein, Gly-

CAM-1 from HEC-GlcNAc6ST<sup>-/-</sup> lymph nodes incorporated  $37.3 \pm 2.7\%$  of the <sup>35</sup>SO<sub>4</sub> compared with GlyCAM-1 from wild-type mice (Fig. 5 B). Additionally, there was an increase in the SDS-PAGE mobility of HEC-GlcNAc6ST<sup>-/-</sup> GlyCAM-1 compared with wild-type GlyCAM-1, consistent with the previous observations obtained with undersulfated GlyCAM-1 (13). CD34 from HEC-GlcNAc6ST<sup>-/-</sup> mice incorporated  $33.8 \pm 2.5\%$  of the <sup>35</sup>SO<sub>4</sub> label compared with wild-type CD34 (Fig. 5 E). These results establish that HEC-GlcNAc6ST is the dominant (but not the exclusive) enzyme contributing to the sulfation of both CD34 and GlyCAM-1, two major components of mouse PNAd.

**MECA79 Reactivity of L-Selectin Ligands in HEC-GlcNAc6ST Null Mice.** To quantify the level of the MECA79 epitope expressed on L-selectin ligands, GlyCAM-1 and CD34 were immunoprecipitated from lymph nodes of wild-type and HEC-GlcNAc6ST<sup>-/-</sup> mice with protein-specific antibodies against these components. Proteins were quantified and the MECA79 reactivity was determined by Western blotting. The normalized MECA79 reactivity of GlyCAM-1 derived from null lymph nodes was  $29.9 \pm 10.8\%$  of that found on wild-type GlyCAM-1 (Fig. 5 C). Similarly, CD34 from null mice showed  $25.9 \pm 11.5\%$  of the normalized MECA79 reactivity compared with wild-type CD34 (Fig. 5 F). Fig. 5 G summarizes the relative sulfate incorporation and MECA79 reactivity of lymph node derived GlyCAM-1 and CD34.

In a parallel analysis, we also analyzed GlyCAM-1 from serum. With equal quantities of coated GlyCAM-1 (Fig. 6 A), the relative MECA79 reactivity of serum GlyCAM-1 from HEC-GlcNAc6ST<sup>-/-</sup> mice was  $28.5 \pm 2.8\%$  of that from wild-type mice (Fig. 6 B). This result demonstrated that the normalized MECA79 reactivity of serum GlyCAM-1 paralleled the reactivity of GlyCAM-1 and CD34 purified from lymph nodes. Serum GlyCAM-1 is abundant and easily purified (32) and thus provided us the means to investigate the biochemical and biophysical properties of a PNAd component formed in situ in the presence or absence of HEC-GlcNAc6ST. In an analogous approach, Homeister et al. (12) took advantage of serum GlyCAM-1 to study the contributions of FucT-IV and FucT-VII in the elaboration of lymph node ligands for L-selectin.

**Interaction of GlyCAM-1 from HEC-GlcNAc6ST Null Mice with L-, P-, and E-Selectin.** Using an L-selectin-IgM chimera as a histochemical probe, we previously observed that the lack of HEC-GlcNAc6ST results in the complete loss of luminal staining from lymph node HEV (26). To examine the selectin binding activities of isolated ligands, we purified GlyCAM-1 from the sera of HEC-GlcNAc6ST<sup>-/-</sup> and wild-type mice, coated equivalent levels of the proteins on ELISA plates, and performed binding assays with the L-selectin-IgM chimera. Wild-type-derived GlyCAM-1 demonstrated significant L-selectin reactivity over a range of chimera concentrations (Fig. 6 C), whereas GlyCAM-1 from HEC-GlcNAc6ST<sup>-/-</sup> mice was completely unreactive at all chimera concentrations.

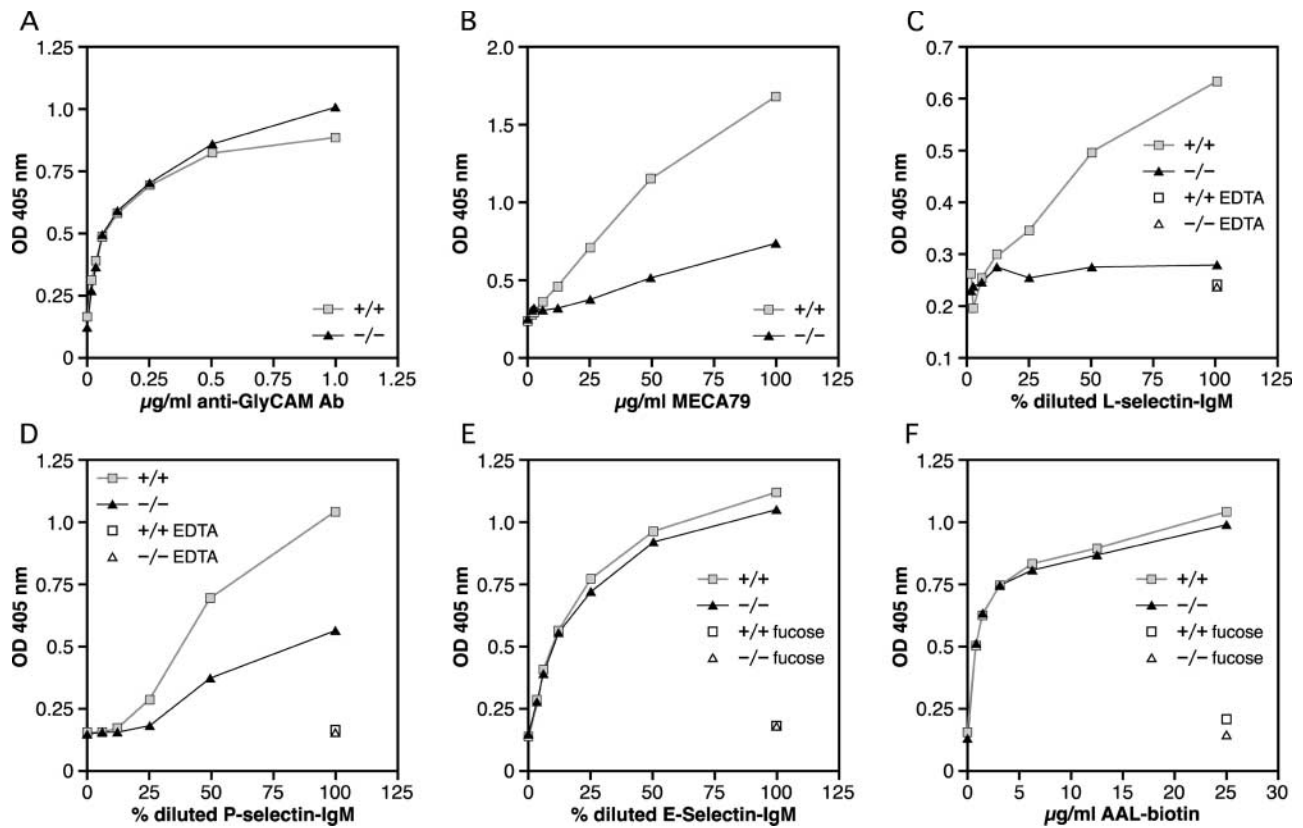


**Figure 6.** ELISA analyses of GlyCAM-1 from HEC-GlcNAc6ST<sup>-/-</sup> mice. Equivalent amounts of HEC-GlcNAc6ST<sup>-/-</sup> and +/+ GlyCAM-1 were coated on ELISA plates. (A) Protein was quantified using an anti-GlyCAM-1 Ab. (B) Relative MECA79 reactivity. L-selectin-IgM (C), P-selectin-IgM (D), or E-selectin-IgM (E) chimeric proteins or biotinylated-AAL (F) were allowed to bind and were subsequently detected with an alkaline phosphatase-conjugated secondary Ab. EDTA (selectins) or fucose (AAL) was used to show specificity of the respective interactions. Plots are representative of three experiments performed on two independent preparations of GlyCAM-1.

The binding of P-selectin-IgM to GlyCAM-1 from null mice was also significantly diminished compared with its binding to wild-type GlyCAM-1 (Fig. 6 D). We also tested E-selectin, whose binding to ligands is dependent on both sialic acid and fucose but independent of sulfation (21). As shown in Fig. 6 E, E-selectin-IgM bound equivalently to GlyCAM-1 from +/+ and -/- mice (Fig. 6 E). Similarly, a lectin from *Aleuria aurantia* (AAL) that preferentially binds  $\alpha$ 1,3-linked fucose bound equivalently to the two forms of GlyCAM-1 (Fig. 6 F).

**Lymphocyte Rolling on GlyCAM-1 from HEC-GlcNAc6ST Null Mice.** To augment our biochemical analysis, we investigated the biophysical characteristics of isolated ligands in a parallel plate flow chamber. The flow chamber provides a means to determine parameters of rolling interactions under physiologic conditions of shear stress. We coated equal amounts of GlyCAM-1 purified from the sera of HEC-GlcNAc6ST<sup>-/-</sup> and +/+ mice onto plates and assessed their ability to support rolling of human L-selectin-expressing Jurkat T cells. Although rolling on GlyCAM-1 from HEC-GlcNAc6ST<sup>-/-</sup> mice was observed, significantly fewer cells rolled stably over a range of shear stresses as compared with rolling on wild-type protein (Fig. 7 A). GlyCAM-1 from null mice also exhibited a marked

decrease in the strength of rolling adhesion, with no interaction evident at shear stresses  $>8$  dyn/cm<sup>2</sup>. Rolling on either form of GlyCAM-1 was confirmed to be L-selectin dependent, as it was completely inhibited by the addition of EDTA or the function-blocking monoclonal antibody DREG56 (Fig. 7, legend). Treatment of either form of coated GlyCAM-1 with sialidase also completely inhibited rolling, confirming that the L-selectin interaction was sialic acid dependent (Fig. 7, legend). Rolling was substantially faster on GlyCAM-1 from HEC-GlcNAc6ST<sup>-/-</sup> (1.6-fold higher at a shear stress of 1 dyn/cm<sup>2</sup>) (Fig. 7 B).

Given that MECA79 had no effect on lymphocyte rolling in HEV of HEC-GlcNAc6ST<sup>-/-</sup> mice *in vivo*, we wanted to determine if GlyCAM-1 purified from HEC-GlcNAc6ST<sup>-/-</sup> mice retained sensitivity to MECA79 inhibition. In striking contrast to the complete lack of effect *in vivo*, MECA79 strongly inhibited rolling on GlyCAM-1 purified from HEC-GlcNAc6ST<sup>-/-</sup> mice with  $>85\%$  inhibition at 1  $\mu$ g/ml of MECA79 (Fig. 7 C). Over a range of MECA79 concentrations (1–10  $\mu$ g/ml), the degree of inhibition of HEC-GlcNAc6ST<sup>-/-</sup> GlyCAM-1 was equivalent to that seen with wild-type GlyCAM-1. In a further experiment, 10  $\mu$ g/ml of MECA79 was applied to varying concentrations of coated HEC-

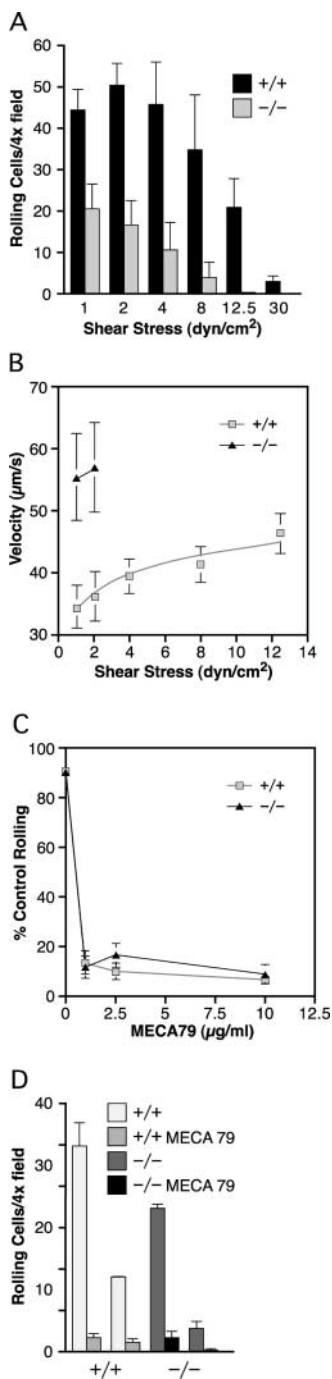


**Figure 7.** Jurkat cell rolling on GlyCAM-1. (A) Equivalent amounts of HEC-GlcNAc6ST<sup>-/-</sup> and +/+ GlyCAM-1 were coated on dishes. Jurkat cells were perfused through the flow chamber and the number of rolling cells was determined for each shear stress. Values represent the mean  $\pm$  SD. Addition of EDTA, mAb DREG56, or sialidase treatment of <sup>-/-</sup> and +/+ GlyCAM-1 inhibited >95% of rolling. The experiment shown is representative of three independent experiments each performed in duplicate using two different fields of view. (B) The velocity of 40 rolling cells was determined for each shear stress. Values represent the mean  $\pm$  SD. (C) GlyCAM-1 from HEC-GlcNAc6ST<sup>-/-</sup> and +/+ mice was coated such that nearly equivalent numbers of rolling cells were observed at wall shear stress of 1–2 dyn/cm<sup>2</sup>. Dishes were treated with varying concentrations of MECA79 mAb and rolling of Jurkat T cells was determined. Data was normalized based on the number of cells that rolled in the absence of mAb. Data shown is for a shear stress of 1 dyn/cm<sup>2</sup>. (D) Varying concentrations of GlyCAM-1 from HEC-GlcNAc6ST<sup>+/+</sup> and <sup>-/-</sup> mice were coated yielding two different levels of rolling for each form of GlyCAM-1. The effect of 10  $\mu$ g/ml of MECA79 on rolling was determined for each type and concentration of GlyCAM-1. Values represent the mean  $\pm$  SD for shear stress of 1 dyn/cm<sup>2</sup>.

GlcNAc6ST<sup>-/-</sup> and +/+ GlyCAM-1 that supported either high or low levels of rolling. Inhibition of rolling was equivalent ( $\sim$ 90%) for both forms of GlyCAM-1 at all concentrations tested (Fig. 7 D). A similar pattern of inhibition with MECA79 was observed when 38C13 cells, a cell line expressing murine L-selectin, were used to test rolling on HEC-GlcNAc6ST<sup>-/-</sup> and +/+ GlyCAM-1. Although a higher concentration of MECA79 was necessary to achieve inhibition with these cells, equivalent inhibition was observed on both types of GlyCAM-1 (unpublished data).

## Discussion

Our initial characterization of HEC-GlcNAc6ST<sup>-/-</sup> mice revealed a marked phenotype with decreased lymphocyte homing and reduced lymphocyte numbers in peripheral lymph nodes (26). The observation that the 50% residual homing in these animals continues to be L-selectin dependent prompted our investigation of the L-selectin ligands that function in the absence of HEC-GlcNAc6ST.

To directly observe the effect of deletion of HEC-GlcNAc6ST on the rolling of lymphocytes in peripheral lymph node HEV, we employed intravital microscopy. We found no difference in the lymphocyte rolling fraction between HEC-GlcNAc6ST<sup>-/-</sup> and +/+ mice, but a substantial defect in lymphocyte sticking in fourth and fifth order venules of HEC-GlcNAc6ST<sup>-/-</sup> mice. Measurement of the velocity of rolling cells revealed a dramatic (fourfold) increase in rolling velocity in fourth order venules. It is plausible that this increase in rolling velocity in the null mice explains the observed defect in lymphocyte sticking in higher order venules; that is, the increase in rolling velocity may decrease the efficiency of chemokine signaling by decreasing the time of exposure of rolling cells to endothelial-associated chemokines. Analogously, when  $\alpha$ 4 $\beta$ 7 integrin function is blocked or genetically inactivated, the velocity of lymphocyte rolling in HEV of Peyer's patches increases dramatically and sticking is greatly reduced (35). Sulfated carbohydrates have been shown to bind chemokines, such as CCL21 (36), whose presentation on the luminal surface of HEV is essential to induce sticking of rolling T cells (37). Thus, it is conceivable that undersulfation of molecules on the luminal surface of HEV in HEC-GlcNAc6ST<sup>-/-</sup> mice may reduce the presentation of CCL21 in high order venules, thus contributing to the observed defect in lymphocyte sticking. Undersulfation of ligands could also affect sticking by diminishing outside-in signaling processes dependent on L-selectin ligand engagement (38).

We have confirmed here that HEC-GlcNAc6ST<sup>-/-</sup> mice have dramatically reduced levels of luminal reactivity for MECA79 in lymph node HEV. Consistent with this observation, neither *in vivo* homing to peripheral lymph nodes nor lymphocyte rolling on HEV was affected by administration of MECA79 mAb to the null animals. Yet, rolling of lymphocytes on HEV remained L-selectin dependent. These observations provide a direct demonstration of the existence of one or more MECA79-unreactive ligand(s) for L-selectin that function(s) in lymph node HEV in the absence of HEC-GlcNAc6ST.

To investigate the L-selectin ligands present in HEC-GlcNAc6ST<sup>-/-</sup> mice, we focused on components of the PNAd complex. We purified GlyCAM-1, a secreted peripheral membrane protein, and CD34, a type I transmembrane protein, from lymph nodes. CD34 has been shown by EM immunocytochemical studies to be predominantly on the luminal surface of blood vessels (8). GlyCAM-1 and CD34 purified from lymph nodes were significantly undersulfated in HEC-GlcNAc6ST<sup>-/-</sup> mice, incorporating 65% less sulfate on a per mass basis than the same ligands



purified from wild-type mice. Consistent with the direct sulfation measurements, a similar decrease was seen in the reactivity of these ligands with the sulfation-dependent antibody MECA79. Analysis of acid hydrolysates of GlyCAM-1 from HEC-GlcNAc6ST<sup>-/-</sup> mice indicated that GlcNAc-6-SO<sub>4</sub> was the predominant (>75% of the total) sulfated saccharide present (unpublished data). Furthermore, the ligand activity of HEC-GlcNAc6ST<sup>-/-</sup> GlyCAM-1 was blocked by MECA79, which requires GlcNAc-6-SO<sub>4</sub> for binding (25). Therefore, we conclude that the residual ligand activity of GlyCAM-1 is dependent on the GlcNAc-6-SO<sub>4</sub> modification rather than other sulfation modifications.

We wanted to confirm that the defect in HEC-GlcNAc6ST<sup>-/-</sup> mice was restricted to sulfation and did not secondarily affect sialylation or fucosylation of ligands. The E-selectin-IgM binding results demonstrated that the sLex moiety was present to equivalent levels on GlyCAM-1 from both types of mice. Equivalent binding by the fucose-specific lectin AAL was further evidence that fucosylation of GlyCAM-1 was not perturbed in HEC-GlcNAc6ST<sup>-/-</sup> mice. In contrast, GlyCAM-1 from HEC-GlcNAc6ST<sup>-/-</sup> mice was unable to support binding of L-selectin-IgM and was also defective in P-selectin-IgM binding. These results demonstrated that this GlyCAM-1 was selectively deficient in the sulfate modification critical for L-selectin and, to a lesser degree, P-selectin binding. P-selectin on activated platelets has previously been shown to recognize the posttranslational modifications of PNAd and to mediate platelet binding to HEV (39). MECA79 treatment substantially reduced the interaction of platelets with HEV, suggesting that the recognition determinant for L- and P-selectin on PNAd are shared. Our result demonstrated that P-selectin is less stringent than L-selectin in its dependency on the GlcNAc-6-sulfate modification generated by HEC-GlcNAc6ST.

Although GlyCAM-1 from HEC-GlcNAc6ST<sup>-/-</sup> mice was unable to bind L-selectin in a stringent equilibrium binding assay, we wanted to observe its activity in the flow chamber, a more sensitive assay to determine perturbations in the formation and dissociation of bonds between L-selectin and its ligands. GlyCAM-1 from null animals was able to support lymphocyte rolling, but significantly fewer cells rolled over a range of shear stresses. Rolling velocities were significantly increased and the strength of rolling adhesions was greatly diminished. Since GlyCAM-1 from HEC-GlcNAc6ST<sup>-/-</sup> mice appears to be modified with sialic acid and fucose at levels equivalent to wild-type, the observed increase in rolling velocity and decrease in shear resistance in the flow chamber is most likely the consequence of the defect in sulfation.

The presence of GlcNAc-6-SO<sub>4</sub> and MECA79 reactivity on GlyCAM-1 and CD34 in the absence of HEC-GlcNAc6ST indicates that a second HEV-expressed GlcNAc-6-sulfotransferase modifies components of PNAd and is capable of creating the MECA79 epitope. A strong candidate for this enzyme is GlcNAc6ST which is expressed at the mRNA level within murine lymph node

HEC (40). This enzyme can participate in the generation of both the 6-sulfo-sLex epitope (19, 24) and the MECA79 epitope (24) in transfected cells.

A decrease in the GlcNAc-6-sulfation of ligands like GlyCAM-1 and CD34 could conceivably explain the increased rolling velocity that we observed by intravital microscopy in higher order venules of HEC-GlcNAc6ST<sup>-/-</sup> lymph nodes. Indeed, we confirmed that undersulfated GlyCAM-1 supports faster rolling in the flow chamber. However, our MECA79 inhibition results argue that these observations are not simply attributable to diminished sulfation of PNAd components. While MECA79 completely inhibited *in vitro* rolling on null mice-derived GlyCAM-1 over a range of ligand concentrations, we observed no effect of this antibody on *in vivo* homing, rolling, or lymphocyte arrest in lymph nodes of the null mice. It is possible GlyCAM-1 from HEC-GlcNAc6ST null mice does not accurately reflect the altered posttranslational modifications of CD34 and other integral membrane components of PNAd and therefore is not an appropriate surrogate of the PNAd-adhesive complex in these mice. Countering this possibility, we observed the same reductions in overall sulfation and the expression of the MECA79 epitope on both GlyCAM-1 and CD34 when HEC-GlcNAc6ST was absent. Therefore, we believe that the deficiency in the ligand activity of null mice-derived GlyCAM-1, as well as its susceptibility to inhibition by MECA79, applies to other members of the PNAd complex. If this generalization is valid, then the contrasting efficacies of MECA79 *in vivo* and *in vitro* in the null mice would argue for the existence of MECA79-unreactive ligands that become functionally predominant in the absence of HEC-GlcNAc6ST. We proposed such ligand activity and termed it "class 2" in our initial characterization of HEC-GlcNAc6ST null animals (26). The present findings indicate that the class 2 ligand is based on a novel protein scaffold with distinctive posttranslational modifications. Furthermore, since MECA79 treatment potently inhibits rolling in wild-type lymph nodes and does not recapitulate the faster rolling we observed in HEC-GlcNAc6ST<sup>-/-</sup> mice, our results imply that the class 2 ligand is up-regulated in higher order venules of HEC-GlcNAc6ST<sup>-/-</sup> mice.

A MECA79-unreactive L-selectin ligand is expressed in HEV of Peyer's patches. This ligand supports fast rolling and is essential to the homing of lymphocytes to this organ (41, 35). Interestingly, the pattern of MECA79 staining of HEC-GlcNAc6ST<sup>-/-</sup> lymph nodes is reminiscent of that seen in Peyer's patches, a tissue in which HEC-GlcNAc6ST is not expressed (19). MECA79 reactivity is apparent only on the abluminal aspect of the HEV of wild-type Peyer's patches, consistent with the inability of MECA79 to block homing to this organ (3). MAdCAM-1 is proposed to be the predominant L-selectin ligand in HEV of Peyer's patches, in addition to its function as a counter receptor for  $\alpha 4\beta 7$  (35). However, we have not observed an up-regulation of MAdCAM-1 expression in lymph nodes of HEC-GlcNAc6ST<sup>-/-</sup> mice (26).

Additional class 2 ligand candidates are those that support rolling of lymphocytes on HEV of frozen sections of human tonsils following treatment of the sections with the mucin degrading enzyme OSGE (42). This ligand is not blocked by MECA79, although it has reactivity with sLex-specific mAbs. Further evidence for diversity in ligands for L-selectin in human lymphoid tissues comes from studies of Michie et al. (43). These investigators found that MECA79 inhibits the adhesion of an L-selectin<sup>+</sup> lymphoma cell line to HEV of human peripheral nodes by only 41%. The diversity of carbohydrate determinants on PNAd components has been demonstrated using a panel of monoclonal antibodies that differentially stain human lymphoid tissues and variably cross-block MECA79 (44). Tu et al. (45) have described a MECA79-unreactive, sulfate and sialic acid-dependent L-selectin ligand which is expressed on human endothelial cells in culture. In contrast, cytokine-activated cardiac microvascular cells express a sulfate dependent ligand that is sialidase insensitive (46). Additionally, a heparan-sulfate-based ligand for L-selectin has been detected on the cell surface of cultured aortic endothelial cells (47). In vivo, a MECA79-unreactive L-selectin ligand is induced on venules in a model of dermal inflammation in the mouse (48). Intravital microscopic studies have revealed L-selectin ligand activity in mesenteric venules of rat and rabbit after surgical exteriorization (49, 50) and in venules of the cremaster muscle of mouse following cytokine treatment (51). Recent studies indicate that this cremaster ligand activity is due to leukocyte-derived PSGL-1 (52).

Future efforts should be directed at identification of the class 2 ligand within lymph nodes and the nature of its posttranslational modifications. Parallel studies (53) indicate the existence of a class 2 ligand (i.e., MECA79 unreactive) on medullary venules (order 1 and 2) within lymph nodes of wild-type mice. Whether this ligand corresponds to the herein described ligand that is up-regulated in the higher order venules of HEC-GlcNAc6ST null mice remains to be determined.

We are grateful to Mark Singer and Stefan Hemmerich for advice. We thank Dr. Lloyd Stoolman for providing the E-selectin-IgM and P-selectin-IgM chimeras.

This research was supported by National Institutes of Health grants GM57411 and R376M23547 (S.D. Rosen), HL54936 and HL62524 (U. von Andrian). A. van Zante is supported by the Medical Scientist Training Program.

Submitted: 14 January 2003

Revised: 18 August 2003

Accepted: 28 August 2003

## References

- Butcher, E.C., and L.J. Picker. 1996. Lymphocyte homing and homeostasis. *Science*. 272:60–66.
- Springer, T.A. 1994. Traffic signals for lymphocyte recirculation and leukocyte emigration: the multistep paradigm. *Cell*. 76:301–314.
- Streeter, P.R., B.T. Rouse, and E.C. Butcher. 1988. Immunohistologic and functional characterization of a vascular ad-

- dressin involved in lymphocyte homing into peripheral lymph nodes. *J. Cell Biol.* 107:1853–1862.
- Puri, K.D., E.B. Finger, G. Gaudernack, and T.A. Springer. 1995. Sialomucin CD34 is the major L-selectin ligand in human tonsil high endothelial venules. *J. Cell Biol.* 131:261–270.
- Sassetti, C., K. Tangemann, M.S. Singer, D.B. Kershaw, and S.D. Rosen. 1998. Identification of podocalyxin-like protein as a high endothelial venule ligand for L-selectin: parallels to CD34. *J. Exp. Med.* 187:1965–1975.
- Samulowitz, U., A. Kuhn, G. Brachtendorf, R. Nawroth, A. Braun, A. Bankfalvi, W. Bocker, and D. Vestweber. 2002. Human endomucin: distribution pattern, expression on high endothelial venules, and decoration with the MECA-79 epitope. *Am. J. Pathol.* 160:1669–1681.
- Rosen, S.D. 1999. Endothelial ligands for L-selectin: from lymphocyte recirculation to allograft rejection. *Am. J. Pathol.* 155:1013–1020.
- Fina, L., H.V. Molgaard, D. Robertson, N.J. Bradley, P. Monaghan, D. Delia, D.R. Sutherland, M.A. Baker, and M.F. Greaves. 1990. Expression of the CD34 gene in vascular endothelial cells. *Blood*. 75:2417–2426.
- Kikuta, A., and S.D. Rosen. 1994. Localization of ligands for L-selectin in mouse peripheral lymph node high endothelial cells by colloidal gold conjugates. *Blood*. 84:3766–3775.
- Rosen, S.D., M.S. Singer, T.A. Yednock, and L.M. Stoolman. 1985. Involvement of sialic acid on endothelial cells in organ-specific lymphocyte recirculation. *Science*. 228:1005–1007.
- Rosen, S.D., S.I. Chi, D.D. True, M.S. Singer, and T.A. Yednock. 1989. Intravenously injected sialidase inactivates attachment sites for lymphocytes on high endothelial venules. *J. Immunol.* 142:1895–1902.
- Homeister, J.W., A.D. Thall, B. Petryniak, P. Maly, C.E. Rogers, P.L. Smith, R.J. Kelly, K.M. Gersten, S.W. Askari, G. Cheng, et al. 2001. The  $\alpha(1,3)$ fucosyltransferases FucT-IV and FucT-VII exert collaborative control over selectin-dependent leukocyte recruitment and lymphocyte homing. *Immunity*. 15:115–126.
- Imai, Y., L.A. Lasky, and S.D. Rosen. 1993. Sulphation requirement for GlyCAM-1, an endothelial ligand for L-selectin. *Nature*. 361:555–557.
- Hemmerich, S., E.C. Butcher, and S.D. Rosen. 1994. Sulfation-dependent recognition of high endothelial venules (HEV)-ligands by L-selectin and MECA 79, and adhesion-blocking monoclonal antibody. *J. Exp. Med.* 180:2219–2226.
- Hemmerich, S., C.R. Bertozzi, H. Leffler, and S.D. Rosen. 1994. Identification of the sulfated monosaccharides of GlyCAM-1, an endothelial-derived ligand for L-selectin. *Biochemistry*. 33:4820–4829.
- van Zante, A., and S.D. Rosen. 2003. Sulphated endothelial ligands for L-selectin in lymphocyte homing and inflammation. *Biochem. Soc. Trans.* 31:313–317.
- Hemmerich, S., H. Leffler, and S.D. Rosen. 1995. Structure of the O-glycans in GlyCAM-1, an endothelial-derived ligand for L-selectin. *J. Biol. Chem.* 270:12035–12047.
- Mitsuoka, C., M. Sawada-Kasugai, K. Ando-Furui, M. Izawa, H. Nakanishi, S. Nakamura, H. Ishida, M. Kiso, and R. Kannagi. 1998. Identification of a major carbohydrate capping group of the L-selectin ligand on high endothelial venules in human lymph nodes as 6-sulfo sialyl Lewis X. *J. Biol. Chem.* 273:11225–11233.
- Bistrup, A., S. Bhakta, J.K. Lee, Y.Y. Belov, M.D. Gunn,

- F.R. Zuo, C.C. Huang, R. Kannagi, S.D. Rosen, and S. Hemmerich. 1999. Sulfotransferases of two specificities function in the reconstitution of high endothelial cell ligands for L-selectin. *J. Cell Biol.* 145:899–910.
20. Hiraoka, N., B. Petryniak, J. Nakayama, S. Tsuboi, M. Suzuki, J.C. Yeh, D. Izawa, T. Tanaka, M. Miyasaka, J.B. Lowe, and M. Fukuda. 1999. A novel, high endothelial venule-specific sulfotransferase expresses 6-sulfo sialyl Lewis(x), an L-selectin ligand displayed by CD34. *Immunity.* 11:79–89.
  21. Tangemann, K., A. Bistrup, S. Hemmerich, and S.D. Rosen. 1999. Sulfation of a high endothelial venule-expressed ligand for L-selectin. Effects on tethering and rolling of lymphocytes. *J. Exp. Med.* 190:935–942.
  22. von Andrian, U.H. 1996. Intravital microscopy of the peripheral lymph node microcirculation in mice. *Microcirculation.* 3:287–300.
  23. Berg, E.L., M.K. Robinson, R.A. Warnock, and E.C. Butcher. 1991. The human peripheral lymph node vascular addressin is a ligand for LECAM-1, the peripheral lymph node homing receptor. *J. Cell Biol.* 114:343–349.
  24. Kimura, N., C. Mitsuoka, A. Kanamori, N. Hiraiwa, K. Uchimura, T. Muramatsu, T. Tamatani, G.S. Kansas, and R. Kannagi. 1999. Reconstitution of functional L-selectin ligands on a cultured human endothelial cell line by cotransfection of  $\alpha 1\rightarrow 3$  fucosyltransferase VII and newly cloned GlcNAc $\beta$ :6-sulfotransferase cDNA. *Proc. Natl. Acad. Sci. USA.* 96:4530–4535.
  25. Yeh, J.C., N. Hiraoka, B. Petryniak, J. Nakayama, L.G. Elies, D. Rabuka, O. Hindsgaul, J.D. Marth, J.B. Lowe, and M. Fukuda. 2001. Novel sulfated lymphocyte homing receptors and their control by a Core1 extension  $\beta 1,3$ -N-acetylglucosaminyltransferase. *Cell.* 105:957–969.
  26. Hemmerich, S., A. Bistrup, M.S. Singer, A. van Zante, J.K. Lee, D. Tsay, M. Peters, J.L. Carminati, T.J. Brennan, K. Carver-Moore, et al. 2001. Sulfation of L-selectin ligands by an HEV-restricted sulfotransferase regulates lymphocyte homing to lymph nodes. *Immunity.* 15:237–247.
  27. Warnock, R.A., S. Askari, E.C. Butcher, and U.H. von Andrian. 1998. Molecular mechanisms of lymphocyte homing to peripheral lymph nodes. *J. Exp. Med.* 187:205–216.
  28. von Andrian, U.H., and C. M'Rini. 1998. In situ analysis of lymphocyte migration to lymph nodes. *Cell Adhes. Commun.* 6:85–96.
  29. Pries, A.R. 1988. A versatile video image analysis system for microcirculatory research. *Int. J. Microcirc. Clin. Exp.* 7:327–345.
  30. Lasky, L.A., M.S. Singer, D. Dowbenko, Y. Imai, W.J. Henzel, C. Grimley, C. Fennie, N. Gillett, S.R. Watson, and S.D. Rosen. 1992. An endothelial ligand for L-selectin is a novel mucin-like molecule. *Cell.* 69:927–938.
  31. Baumhueter, S., M.S. Singer, W. Henzel, S. Hemmerich, M. Renz, S.D. Rosen, and L.A. Lasky. 1993. Binding of L-selectin to the vascular sialomucin CD34. *Science.* 262:436–438.
  32. Singer, M.S., and S.D. Rosen. 1996. Purification and quantification of L-selectin-reactive GlyCAM-1 from mouse serum. *J. Immunol. Methods.* 196:153–161.
  33. Maly, P., A. Thall, B. Petryniak, C.E. Rogers, P.L. Smith, R.M. Marks, R.J. Kelly, K.M. Gersten, G. Cheng, T.L. Saunders, et al. 1996. The  $\alpha(1,3)$ fucosyltransferase Fuc-TVII controls leukocyte trafficking through an essential role in L-, E-, and P-selectin ligand biosynthesis. *Cell.* 86:643–653.
  34. Tangemann, K., M.D. Gunn, P. Gibling, and S.D. Rosen. 1998. A high endothelial cell-derived chemokine induces rapid, efficient, and subset-selective arrest of rolling T lymphocytes on a reconstituted endothelial substrate. *J. Immunol.* 161:6330–6337.
  35. Bargatze, R.F., M.A. Jutila, and E.C. Butcher. 1995. Distinct roles of L-selectin and integrins  $\alpha 4 \beta 7$  and LFA-1 in lymphocyte homing to Peyer's patch-HEV in situ: the multistep model confirmed and refined. *Immunity.* 3:99–108.
  36. Hirose, J., H. Kawashima, M. Swope Willis, T.A. Springer, H. Hasegawa, O. Yoshie, and M. Miyasaka. 2002. Chondroitin sulfate B exerts its inhibitory effect on secondary lymphoid tissue chemokine (SLC) by binding to the C-terminus of SLC. *Biochim. Biophys. Acta.* 1571:219–224.
  37. Stein, J.V., A. Rot, Y. Luo, M. Narasimhaswamy, H. Nakanishi, M.D. Gunn, A. Matsuzawa, E.J. Quackenbush, M.E. Dorf, and U.H. von Andrian. 2000. The CC chemokine thymus-derived chemotactic agent 4 (TCA-4, secondary lymphoid tissue chemokine, 6CKine, exodus-2) triggers lymphocyte function-associated antigen 1-mediated arrest of rolling T lymphocytes in peripheral lymph node high endothelial venules. *J. Exp. Med.* 191:61–76.
  38. Hwang, S.T., M.S. Singer, P.A. Gibling, T.A. Yednock, K.B. Bacon, S.I. Simon, and S.D. Rosen. 1996. GlyCAM-1, a physiologic ligand for L-selectin, activates beta 2 integrins on naive peripheral lymphocytes. *J. Exp. Med.* 184:1343–1348.
  39. Diacovo, T.G., K.D. Puri, R.A. Warnock, T.A. Springer, and U.H. von Andrian. 1996. Platelet-mediated lymphocyte delivery to high endothelial venules. *Science.* 273:252–255.
  40. Uchimura, K., H. Muramatsu, K. Kadomatsu, Q.W. Fan, N. Kurosawa, C. Mitsuoka, R. Kannagi, O. Habuchi, and T. Muramatsu. 1998. Molecular cloning and characterization of an N-acetylglucosamine-6-O-sulfotransferase. *J. Biol. Chem.* 273:22577–22583.
  41. Kunkel, E.J., C.L. Ramos, D.A. Steeber, W. Müller, N. Wagner, T.F. Tedder, and K. Ley. 1998. The roles of L-selectin, beta 7 integrins, and P-selectin in leukocyte rolling and adhesion in high endothelial venules of Peyer's patches. *J. Immunol.* 161:2449–2456.
  42. Clark, R.A., R.C. Fuhlbrigge, and T.A. Springer. 1998. L-Selectin ligands that are O-glycoprotease resistant and distinct from MECA-79 antigen are sufficient for tethering and rolling of lymphocytes on human high endothelial venules. *J. Cell Biol.* 140:721–731.
  43. Michie, S.A., P.R. Streeter, P.A. Bolt, E.C. Butcher, and L.J. Picker. 1993. The human peripheral lymph node vascular addressin. An inducible endothelial antigen involved in lymphocyte homing. *Am. J. Pathol.* 143:1688–1698.
  44. Berg, E.L., A.T. Mullenney, D.P. Andrew, J.E. Goldberg, and E.C. Butcher. 1998. Complexity and differential expression of carbohydrate epitopes associated with L-selectin recognition of high endothelial venules. *Am. J. Pathol.* 152:469–477.
  45. Tu, L., M.D. Delahunty, H. Ding, F.W. Luscinskas, and T.F. Tedder. 1999. The cutaneous lymphocyte antigen is an essential component of the L-selectin ligand induced on human vascular endothelial cells. *J. Exp. Med.* 189:241–252.
  46. Zakrzewicz, A., M. Grafe, D. Terbeek, M. Bongrazio, W. Auch-Schwelk, B. Walzog, K. Graf, E. Fleck, K. Ley, and P. Gaehtgens. 1997. L-selectin-dependent leukocyte adhesion to microvascular but not to macrovascular endothelial cells of the human coronary system. *Blood.* 89:3228–3235.
  47. Giuffrè, L., A.S. Cordey, N. Monai, Y. Tardy, M. Schapira, and O. Spertini. 1997. Monocyte adhesion to activated aortic

- endothelium: role of L-selectin and heparan sulfate proteoglycans. *J. Cell Biol.* 136:945–956.
48. Hirata, T., B.C. Furie, and B. Furie. 2002. P-, E-, and L-selectin mediate migration of activated CD8(+) T lymphocytes into inflamed skin. *J. Immunol.* 169:4307–4313.
  49. von Andrian, U.H., J.D. Chambers, L.M. McEvoy, R.F. Bargatze, K.E. Arfors, and E.C. Butcher. 1991. Two-step model of leukocyte-endothelial cell interaction in inflammation: distinct roles for LECAM-1 and the leukocyte  $\beta$  2 integrins in vivo. *Proc. Natl. Acad. Sci. USA.* 88:7538–7542.
  50. Ley, K., T.F. Tedder, and G.S. Kansas. 1993. L-selectin can mediate leukocyte rolling in untreated mesenteric venules in vivo independent of E- or P-selectin. *Blood.* 82:1632–1638.
  51. Jung, U., C.L. Ramos, D.C. Bullard, and K. Ley. 1998. Gene-targeted mice reveal importance of L-selectin-dependent rolling for neutrophil adhesion. *Am. J. Physiol.* 274: H1785–H1791.
  52. Sperandio, M., M.L. Smith, S.B. Forlow, T.S. Olson, L. Xia, R.P. McEver, and K. Ley. 2003. P-selectin glycoprotein ligand-1 mediates L-selectin-dependent leukocyte rolling in venules. *J. Exp. Med.* 197:1355–1363.
  53. M'Rini, C., G. Cheng, C. Schweitzer, L.L. Cavanaugh, R.T. Palframan, T.R. Mempel, R.A. Warnock, J.B. Lowe, E.J. Quackenbush, and U.H. von Andrian. 2003. A novel endothelial L-selectin ligand in lymph node medulla that is regulated by  $\alpha$ (1,3)-fucosyltransferase-IV. *J. Exp. Med.* 198: 1301–1312.